Quantifying jellyfish bloom dynamics using aerial surveys and image-based cohort analysis in a Mediterranean lagoon

Marie Meffre, Yann Tremblay, Anaïs Courtet, Etienne Bourgouin, Juan-Carlos Molinero, Delphine Bonnet

Ecological Informatics 95 (2026) 103737

Contents lists available at ScienceDirect

Ecological Informatics

journal homepage: www.elsevier.com/locate/ecolinf

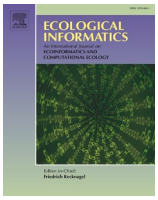

Quantifying jellyfish bloom dynamics using aerial surveys and image-based cohort analysis in a Mediterranean lagoon

Marie Meffre [a,c,*], Yann Tremblay [b], Anaïs Courtet [c], Etienne Bourgouin [c], Juan-Carlos Molinero [b], Delphine Bonnet [a]

[a] MARBEC, Univ. Montpellier, CNRS, Ifremer, IRD, Montpellier, France
[b] MARBEC, IRD, CNRS, Ifremer, Univ. Montpellier, Sète, France
[c] Aquarium de Paris, Paris, France

ARTICLE INFO

Keywords:
Rhizostoma pulmo
Image processing
Plane survey
Population dynamics
Mediterranean Sea
Bages-Sigean lagoon

ABSTRACT

Jellyfish blooms represent a rapid production of huge biomass with many ecological and economic consequences. However, their prediction remains elusive because the scale and dynamics of biomass accumulation are difficult to measure with sufficient spatial and temporal resolution to fully capture their magnitude. Lately, non-invasive biomass estimations based on unmanned aerial surveys of jellyfish distribution have been implemented. However, they generally occur at low altitudes and are not adequate to assess the entire spatial dimension of a jellyfish bloom. In this study, a high-resolution camera was on board of a small plane flying at 300 to 700 m altitude to map the *Rhizostoma pulmo* (Cnidaria; Rhizostomeae) bloom in an entire Mediterranean lagoon (38 km^2), at the beginning (July), the middle (August), and the end (October) of the 2022 event. Based on image analysis tailored algorithms we computed and mapped jellyfish densities and biomass for each flight. The maximum biomass was reached in July (886 t in total, maximum biomass density of 8 kg/100 m^2), followed by August (456 t, maximum biomass density of 3 kg/100 m^2). October displayed the least biomass (401 t, maximum biomass density of 3 kg/100 m^2). This approach provides novel insights of the *R. pulmo* bloom's spatial dimension and details on the jellyfish patchy distribution and temporal changes in population size structure, allowing detecting different cohorts. The aerial survey at high altitude proves to be an efficient method to monitor jellyfish blooms dynamics at coarse scale, although abundance and therefore biomass might be underestimated due to the individuals size detection limits.

1. Introduction

Jellyfish blooms magnitude and frequency seem to have increased during the last decades with significant consequences on ecosystems and economical activities (e.g. Graham et al., 2014; Lee et al., 2023; Richardson et al., 2009). Although jellyfish are often characterized in terms of their negative impacts on fisheries, which can result in annual economic losses of millions of dollars, they also constitute a valuable and largely underexploited bioresource (Uye, 2011; Graham et al., 2014; Brotz, 2016). In South-East Asia, jellyfish, especially Rhizostomeae, have been consumed for over a thousand years and high demand remains nowadays (Brotz et al., 2024). Medusae are also exploited in many other domains such as pharmaceuticals, biotechnologies or aquaculture (D'Ambra and Merquiol, 2022; Duarte et al., 2022; Graham et al., 2014). While medusae fisheries are well established in Asia, their implementation in Europe remains limited so far (Brotz, 2016; Elliott et al., 2017). In the Mediterranean Sea, landings of jellyfish were highly unstable and no formal stock assessment frameworks were in place leading to the collapse of jellyfish fisheries (Brotz, 2016). The 'bloom and burst' nature of jellyfish associated with their patchy distribution makes stocks management complex. Thus, developing efficient methods to rapidly and robustly evaluate the available jellyfish biomass is necessary to understand jellyfish dynamics for ecological and economical purposes.

Jellyfish exhibit a patchy distribution, often forming high-density swarms shaped by winds and currents (Hamner and Dawson, 2009; Fernández-Alías et al., 2024; Nagata et al., 2024). This spatial heterogeneity poses significant challenges for traditional abundance survey techniques, such as net sampling and visual transects from vessels (e.g., Purcell, 2009; Rowe et al., 2022). While these approaches can provide

* Corresponding author at: MARBEC, Univ. Montpellier, CNRS, Ifremer, IRD, Montpellier, France.
E-mail address: marie.meffre@umontpellier.fr (M. Meffre).

https://doi.org/10.1016/j.ecoinf.2026.103737
Received 27 September 2025; Received in revised form 20 March 2026; Accepted 20 March 2026
Available online 22 March 2026

accurate localized estimates, their limited spatial coverage hampers extrapolation to broader scales and can lead to under- or over-estimation of population density. Hence, the development and application of complementary approaches are essential to better capture the spatio-temporal dynamics of jellyfish blooms.

To address such limitations, over the past two decades researchers have developed a range of alternative monitoring techniques, including underwater cameras, LiDAR, sonars, and aerial imagery, sometimes combined with Artificial Intelligence (AI), alongside citizen science initiatives (Churnside et al., 2016; Fleming et al., 2013; Gao et al., 2021; Graham et al., 2003; Han et al., 2022; Kim et al., 2016; Makabe et al., 2012; Mariani, 2018; Ruiz-Frau et al., 2022; Xiaobin et al., 2021). Among these, aerial imaging stands out for its capacity to rapidly survey large spatial extents, making it particularly suitable for detecting mobile or patchily distributed marine organisms (McGeady et al., 2023; Schaub et al., 2018). In parallel, recent progress in high-resolution aerial imagery (e.g. from drones, ultra-light motorized planes or airplanes) had made possible accurate non-invasive morphometric measurements (Gray et al., 2019; Raoult and Gaston, 2018). Planes and drones have been used to monitor a wide range of marine wildlife in the last decades including visual and photography-based observations to quantify jellyfish from the air (Houghton et al., 2006; Purcell et al., 2000; Rowley et al., 2020; Uye et al., 2003), with growing use of automated detection algorithms to reduce the human cost of the analysis (Graham et al., 2003; Hamel et al., 2021; Mcilwaine and Casado, 2021; Raoult and Gaston, 2018; Schaub et al., 2018). Hybrid approaches combining automatic and manual detection have also been explored to evaluate performance trade-offs (Choi et al., 2021; Rowe et al., 2022).

A wide range of medusae have been monitored using aerial methods, from small (mean diameter < 30 cm) transparent medusae (e.g. *Aurelia* spp. de Lamarck, 1816, *Chironex fleckerii* Southcott, 1956) (Hamel et al., 2021; Purcell et al., 2000; Rowley et al., 2020; Schaub et al., 2018; Uye et al., 2003), to larger (mean diameter > 30 cm) more visible species, such as *Catostylus mosaicus* Quoy and Gaimard, 1824-1826, *Cyanea capillata* (Linnaeus, 1758), *Nemopilema nomurai* Kishinouye, 1922, *Phyllorhiza punctata* von Lendenfeld, 1884, *Rhizostoma octopus* (Gmelin, 1791) (Choi et al., 2021; Graham et al., 2003; Houghton et al., 2006; Raoult and Gaston, 2018; Rowe et al., 2022). Large jellyfish (over 30 cm of average diameter) are typically monitored using aerial surveys from planes, as their size allows detection from high altitudes, enabling efficient coverage of vast areas (Graham et al., 2003; Houghton et al., 2006). By contrast, drones offer distinct advantages: they are cost-effective, require minimal logistical support, and operate at low altitudes, which permits higher-resolution imaging and more accurate identification of individual medusae. Nevertheless, their limited flight autonomy currently restricts their capacity to rapidly survey large spatial extents.

In this study, *Rhizostoma pulmo* (Macri, 1778) population dynamics monitoring was conducted in a mediterranean lagoon using aerial surveys. High-resolution imagery, combined with and a robust image analysis algorithm, was employed to (i) quantify jellyfish abundance and estimate total biomass, (ii) characterize size-based cohorts, and (iii) map the spatial distribution and the extent of the bloom across the lagoon. While aerial methods have previously been applied to jellyfish monitoring, our approach provides two key innovations: the estimation of bloom biomass from imagery and the identification of population structure through cohort detection. Beyond ecological monitoring, jellyfish, especially Rhizostomeae, are increasingly recognized as a valuable bioresource, with potential applications in various industries such as pharmaceuticals, food, and biotechnology.

2. Material and methods

2.1. Study site and field sampling sessions

Bages-Sigean lagoon (43°05′12.72″N; 3°00′35.3″E) (Aude, France)

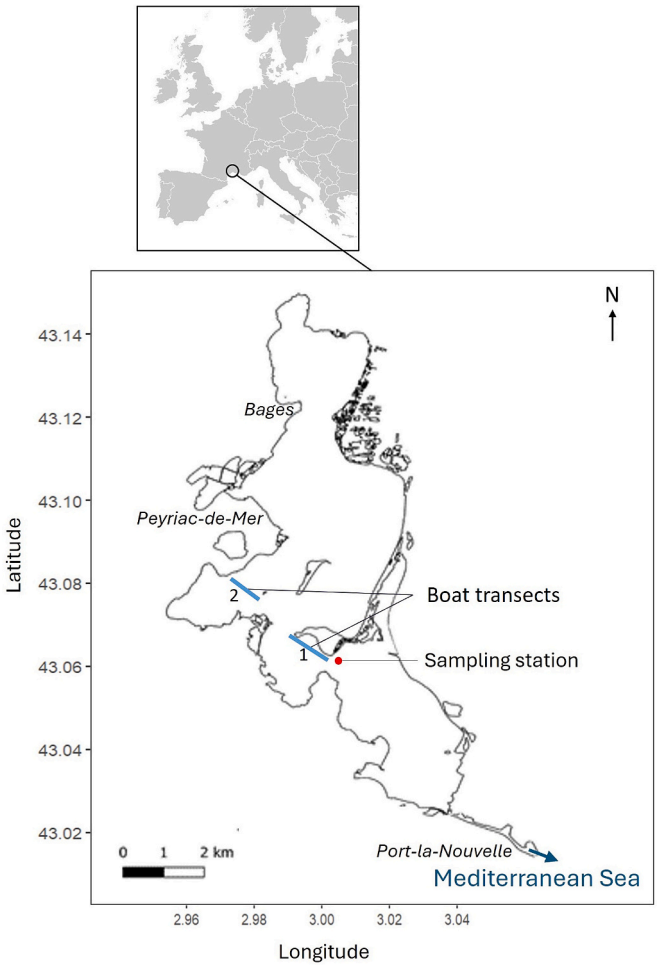

Fig. 1. Location of the boat transects (blue lines), and sampling station (red dot) used for environmental parameters measurements and nets sampling in Bages-Sigean lagoon. (For interpretation of the references to colour in this figure legend, the reader is referred to the web version of this article.)

(Fig. 1) is a semi-enclosed lagoon covering an area of 38 km^2 connected to the Mediterranean Sea through the sea inlet of Port-la-Nouvelle, in the south, and mostly alimented in freshwater and nutrients by the channel of La Robine, in the north. The lagoon is shallow, with maximum and average depths of 4 and 2 m respectively, which allows reliable detection of *R. pulmo* from aerial surveys, even in the deepest areas, as medusae exhibit limited vertical migration. Moreover, the narrow connection with the open sea restricts the exchange of individuals, preventing escape from the lagoon and ensuring that the same population of *R. pulmo* is monitored throughout the study. The lagoon lies within the protected natural park, "Parc Naturel Régional de La Narbonnaise en Méditerranée" and supports both artisanal fisheries of eels and touristic activities. *R. pulmo* is recurrently observed in this lagoon since 2014 (Stéphane Marin personal communication). A previous study from Leoni et al. (2021) has shown that three to four successive cohorts usually occur from June to November in this lagoon.

Temperature and salinity were measured in the lagoon at a single station with a multiparameter probe (Hanna HI 9829) from late March to October 2022. Chlorophyll a was measured following the same method as described in Leoni et al. (2021) (Fig. 1). To account for jellyfish density and biomass, in situ monitoring was conducted in the lagoon simultaneously with the aerial surveys. Boat-based transects of 1 km were performed at two locations, with two observers counting medusae by size class (0–5, 5–10, 10–30 and above 30 cm) within a 3 m-wide corridor on each side of the boat. In addition, net sampling was

conducted at a fixed station (Fig. 1), and random hand-net sampling was used to measure individual medusae total length.

2.2. Aerial surveys

Three flights by airplane (Pipistrel Virus) were carried out, on the 12th of July, 31st of August and 4th of October 2022. Each flight covered the entire lagoon area (Fig. 2). The plane flew at altitudes varying from 140 to 755 m and was equipped with a high-resolution camera (PhaseOne IXA 180 with a Schneider-Kreuznach 55 mm f/2.8) offering resolution of 10,328 × 7660 pixels. At these altitudes, and with this lens, ground resolution varied from 1 to 6 cm, allowing to identify *R. pulmo* individuals (Fig. 3). The camera was set to record an image every two seconds.

2.3. Image treatment

2.3.1. Georeferencing the images

Image georeferencing was conducted based on the method described by Correia et al. (2022). The initial inputs were the geographic coordinates, yaw, pitch (minus 90° as the camera looks down) and roll of the plane, which were used as proxy for those of the camera. Knowing geographic location, altitude, yaw, pitch, roll, and camera lens opening angles (40.2° and 52.0° for the short and long side respectively), the four corners of each image were projected onto the ground, allowing to calculate their geographic coordinates. This, in turn, permitted the calculation of the ground area covered, from which the average pixel-ground size (PGS) for each image was derived. PGS was used to obtain the areas in m^2 from px^2.

2.3.2. Isolating the counting area

Medusae are distinguishable on aerial images as small contiguous bright pixels on darker water background. Unfortunately, other objects can meet these criteria, such as boats, birds, floating objects, and more importantly, sun reflections. A first mask (logical true-false matrix) was calculated based on pixels' brightness in order to flag out these objects. For our dataset, pixels with both red, green and blue values ≥250 (image pixels being coded using 8 bits, i.e. with a maximum of 255) systematically removed all sun reflections, and most of the remaining objects.

The second challenge was to distinguish water from land in images that partially included terrestrial areas. Due to significant variations in lighting conditions and water coloration across the images, colour alone could not be reliable for this purpose. Instead, the differences in uniformity were used to distinguish them. An edge detection algorithm followed by line dilatation and hole filling allowed us to efficiently select pixels belonging to land versus water. Combining these two masks allowed us to delimit the water area within which the jellyfish were detected and quantified (Fig. 3).

2.3.3. Detection of the medusae

R. pulmo medusae appeared as ovoid, slightly elongated light blue-gray spots in the water (Fig. 3). A pixel's brightness threshold followed by a size filter was used to detect the medusae from the background of the lagoon. A size limit threshold was fixed to only detect items between 10 and 40 cm. Ten centimeters (2–10 pixels) represented the minimal size at which a *R. pulmo* medusae could be detected at the flying altitudes of the plane, using a high-resolution camera. Forty centimeters corresponded to the largest total length measured in the individuals sampled from the lagoon in 2022. The PGS of each image was used to transform these metric limits into pixels according to the altitude. The number of detected jellyfish was automatically recorded for each image. An ellipse was drawn around each detected object, the geographic coordinates of the centroid, the major axis length, the area and the eccentricity (ratio between major and minor axis) were measured. Abnormally high values of eccentricity corresponded to floating leaves of seagrass and were removed from the dataset. The major axis lengths were proxies for the total length of the jellyfish and were transformed from pixels to meters by multiplying them with the PGS values.

2.3.4. Waves

Under some specific weather conditions and view angles, small ripples caused by the combined effects of swell and wind resulted in false positives among the detected medusae. Indeed, these bright ripples were not always saturated enough to be removed by the sun glare mask and could thus be detected as jellyfish when they were within the medusae size range. Instead of trying to remove them individually, we rather tried to evaluate if an image was at-risk of being concerned with false positives. This was based on the observation that images with many false positives showed clear parallel lines of clearer and darker alternances following swell frequency and/or wind-mediated patterns on the water surface. More frequent alternances meant more risk. This frequency was measured using a Fourier transform (FFT) on pixel values along a line passing through the center of the image. A peak in FFT magnitude was deemed to occur when considered significant, i.e. when FFT magnitudes exceeded the threshold of the mean plus three times the standard deviation. Since the pattern's orientation could not a-priori be known, this measure was conducted on all the 18 lines every 10°. When the line orientation was most orthogonal to the wave pattern, the Fourier

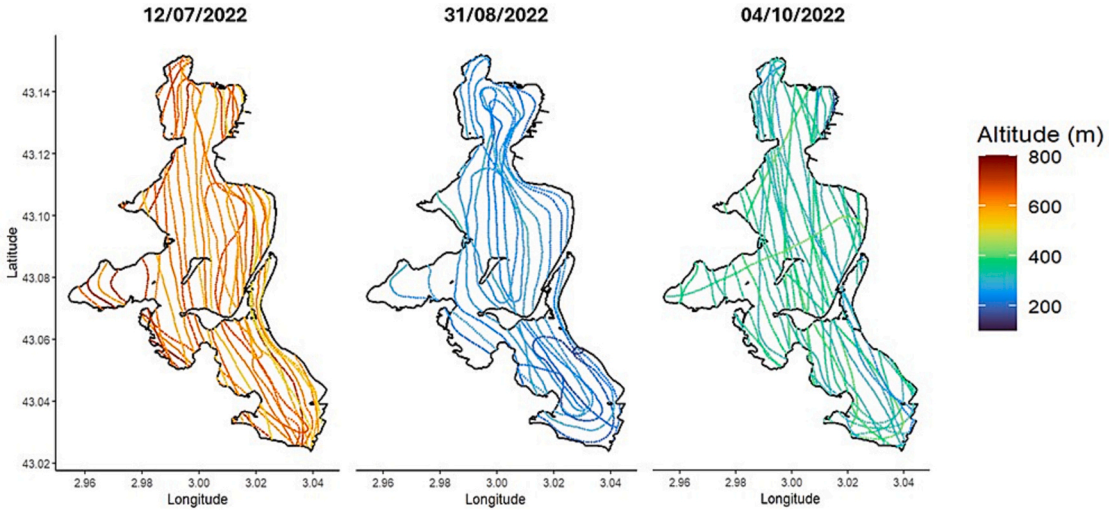

Fig. 2. Trajectory and altitude (m) of the plane during the three flights above Bages-Sigean lagoon on the 12/07/2022, 31/08/2022 and 04/10/2022.

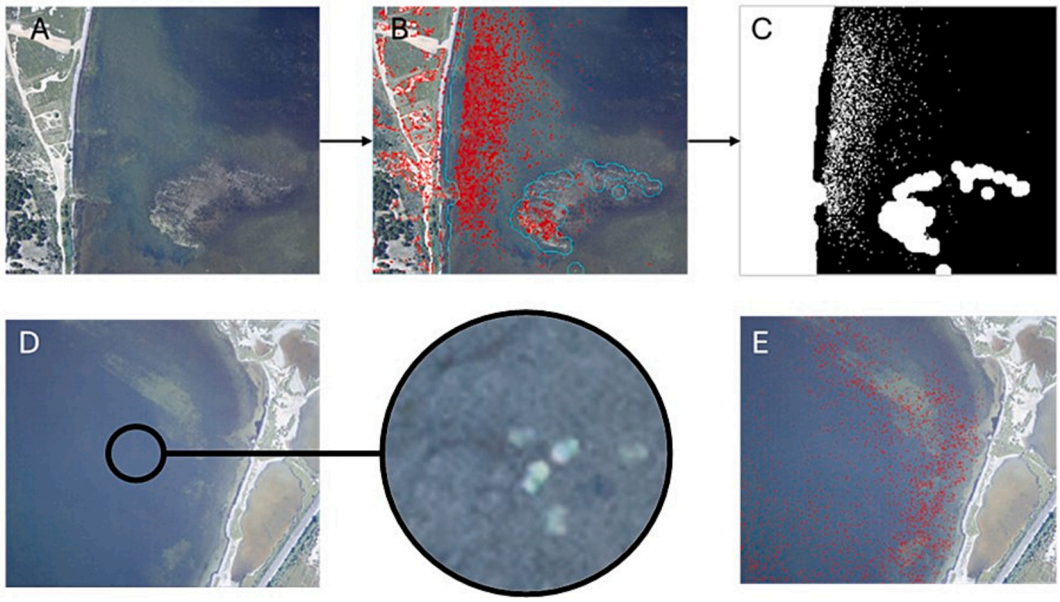

Fig. 3. Process of medusae detection from the images: A = original image, the pixel to ground ratio and the coordinates have been calculated, B = detection and removal of the land (blue) and the sun glare and any other object out of the water (red), C = mask of the area that will be analyzed (in black), the removed objects appear in white, D = another image with medusae, E = detection of the medusae in red. (For interpretation of the references to colour in this figure legend, the reader is referred to the web version of this article.)

transform peak was maximum and then selected as the peak for this image. Absence of peak or low maximum peak value indicated calm sea and low risk, whereas high maximum peak value indicated high risk of false positive in the medusae count.

As a conservative measure, and due to the large volume of data, only images without significant peak or with maximum peaks below the median values of all peaks calculated on the 3 flights were selected, i.e. 1.162×10^{-3}.

2.3.5. Comparison with manual detection of the jellyfish

Jellyfish were manually counted by jellyfish experts on 21 images sampled randomly in the three flights. Each image was counted by two to four different experts. The images were selected for their variation in jellyfish density. Jellyfish in these images were marked with a red dot in an image editor. The final counts were obtained using a code to detect the number of red dots per image. This colour was chosen because it was not naturally present on the images. The results were compared with those obtained automatically.

2.4. Statistical analysis

2.4.1. Biomass per $100m^2$

The biomass was determined for each jellyfish using Leoni et al. (2021) relationship between wet weight and size for *R. pulmo*:

$$WW = 0.19 \times TL^{2.63}$$

Where WW is the wet weight (g) and TL the total length (cm) of the jellyfish.

The biomass per $100m^2$ was then determined by dividing the total biomass of the image (kg) by the area occupied by the water in the image (m^2) and multiplying the result by 100.

2.4.2. Biomass maps

The map of the lagoon was divided into squares of 300mx300m. In each square, the average biomass per $100m^2$ was calculated from all the images which central coordinates fell in the square area. The maps were constructed for each survey date using a shapefile of the lagoon and the packages "sf", "sp" and "ggplot2"in Rstudio. As all the maps were not completely covered by the images, mostly due to the removal of the images with FFT above the median, the maps were interpolated. The interpolation was done using a kriging method which considers borders and has been proven to be efficient for mapping biomass distribution (Oliver and Webster, 1990; Chen et al., 2019). An exponential model was used to calculate the variogram as this model has the lower RSS score and is advised for patchy distribution with sharp edges (Webster and Oliver, 2007). All the grouped statistics were calculated using the package "dplyr" and "gstat" in Rstudio.

2.4.3. Cohorts' detection

A random sample of 10,000 medusae total lengths (cm) was selected for each flight. The sampling and the process of cohorts' detection were repeated three times for each flight to ensure the stability of the results. Cohorts were detected based on the distribution of the sizes frequency. Each cohort corresponds to a fitted lognormal function, the number of gaussian curves that best fits the distribution was determined using the package "Mixdist" in Rstudio. The parameters associated with each cohort distribution (proportion of the cohort in the data, mean and standard deviation values) were used to calculate the probabilities of belonging to each cohort for an individual. The individuals were then associated with the most probable cohort for every dataset. A von Bertalanffy growth function (VBGF) was calculated only for the third cohort. Indeed, individuals of the first cohort had already reached their maximal size in July and, therefore, their growth was not observed in August or October. The second cohort was only detected for two dates, which is not enough to properly estimate medusae growth. Finally, the individuals of the fourth cohort were only observed on the last date of the survey. The asymptotic length (L_{inf}) was fixed at 40 cm, the maximum total length detected during the in situ jellyfish samplings (unpublished results). This parameter had to be fixed because of the limited number of dates, thus only t_0 and the growth coefficient (K) were estimated from the function applied to empirical data. The VBGF function was calculated in Rstudio using the "nlstools" and the "FSA" packages.

3. Results

3.1. Environmental conditions

Temperature in the lagoon varied between 12.3 (end of March) and 26.2 °C (mid-June) (mean = 20.8 ± 5.1 °C) (Fig. 4 A). Salinity increased all along the summer, going from 15.0 at the end of March to 44.5 at the beginning of October (mean = 33.8 ± 8.6) (Fig. 4 B). Chlorophyll a peaked in May (2.17 ± 0.40 µg/L) and was at its lowest in mid-July (0.23 ± 0.02 µg/L); the overall mean was 0.95 ± 0.58 µg/L (Fig. 4 C).

3.2. Flights characteristics

The airplane flew across the entire lagoon during all the flights, nevertheless, variations in the plane altitude and trajectory resulted in differences in the surface area covered. The July and October flights, conducted at higher altitude (mean altitude >300 m) covered the whole lagoon. In contrast, the August flight, flown at a lower altitude (around 260 m), and covered less lagoon surface. Thus, higher altitude is associated with greater coverage of the study site (Fig. 2, Table 1).

More than 2000 images were taken in Bages-Sigean lagoon during each flight (Table 1). The vast majority of them allowed for medusae detections. However, after removing images with significant ripples that could lead to false positives, the number of images used for the maps was just under 2000 for flights 1 and 3, and less than 1000 for flight 2 (Table 1).

Most of the detected jellyfish measured about 30 cm total length. Adult specimens (total length > 15 cm, as defined by Leoni et al. (2021)) represented the majority of detected individuals, even in July. The mean size of jellyfish mean size slightly decreased over time, and the mean weight, calculated from total length measurement, followed the same trend. The highest total biomass in the lagoon was observed in July and decreased in the following months. By October, the total biomass was slightly more than half of the value observed three months earlier (Table 1).

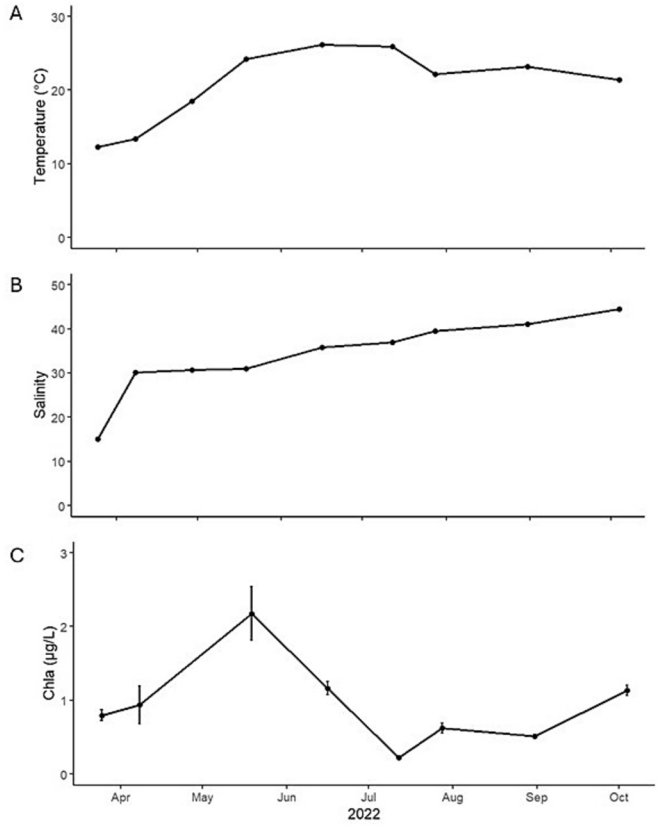

Fig. 4. Temperature (°C), salinity and mean ± sd chlorophyll *a* (µg/L) from Spring to Autumn 2022 in Bages Sigean lagoon (France).

3.3. Automatic vs. manual counts

Medusae were counted manually in 21 images from the three flights to assess the algorithm's performance. The standard error between counters varied from 0 to 1360 jellyfish per picture (Fig. 5). Visual counts significantly differ from automatic counts (Wilcoxon-Mann-Whitney test, *p*-value <0.001) (Fig. 5). The August flight displayed a larger discrepancy compared to the other flights, with many false positives from automatic detection (Fig. 5).

Higher altitudes reduce detection accuracy, as the medusae are less visible, leading to variations in results between automatic and manual detection, as well as between the manual counters (Fig. 5). The removed objects of the mask are surrounded by a buffer, meaning that some medusae near suppressed items, such as sun glare, might be excluded from the analysis. Thus, when large areas are removed from the image, the smaller analyzed area may result in fewer medusae being detected. Additionally, small sun glare spots on ripples can be misidentified as jellyfish by the algorithm. These variables are positively correlated with the difference between manual and automatic counts (Spearman's coefficients of correlation: 0.52 for the FFT peak height, 0.30 for the altitude and 0.20 for the area analyzed). The strongest correlation is with the FFT peak height, which was higher on the flight of August than on the other flights (Fig. 5). The false positives induced by the ripples explain the differences between the visual and automatic counts.

3.4. Medusae biomass

Boat transects occurred simultaneously to flight surveys. *R. pulmo* was only observed during transects carried out on 12/07/2022. Biomass estimates of 0.11 kg per 100 m^2 and 0.02 kg per 100 m^2 were obtained from the two transects (Fig. 1). Individuals under 10 cm contributed up to 2% of the total biomass, while individuals between 10 and 30 cm and above 30 cm represented 74% and 23% respectively of the total biomass. To support size calibration from aerial imagery, individual measurements were obtained in the field. On 12/07/2022, mean jellyfish size was 27.4 ± 4.0 cm (n = 52; range: 19.5–40.0 cm). Similar sizes were observed on 31/08/2022 (28.0 ± 4.1 cm, n = 50), while a decrease in mean size was observed on 04/10/2022 (25.9 ± 6.6 cm, n = 42). No *R. pulmo* were detected in 200 or 700 µm plankton net samples.

As expected, jellyfish were distributed in large patches at all surveyed dates (Fig. 6). The total estimated biomass of medusae in the lagoon was the highest in mid-July (886 t) and decreased progressively through time, being almost halved by late August (459 t). The lowest biomass detected is 401 t in early October (Fig. 6).

In mid-July, two main medusae patches were present in the center part of the lagoon. The patch with the higher biomass density covered an area of about 2.1 km^2 in the West of the lagoon (5.5% of its area). Its density starts at 3 kg/100 m^2 and increase towards the lagoon center until reaching 8 kg/100 m^2. A second major patch was detected in the East of Bages-Sigean lagoon, with a smaller area of 2.4 km^2 (6.3% of the lagoon) and a density from 3 to 5 kg/100 m^2 (Fig. 6). Additionally, a smaller patch (0.6 km^2) with a similar density variation was present in the East of the lagoon. In the southern part of the lagoon, two patches of 0.7 km^2 each exhibited densities ranging from 3 to 4 kg/100 m^2 (Fig. 6).

By the end of August biomass densities were reduced and only one main patch was detected. This patch covered 6.1 km^2 (16.0% of the lagoon), with densities ranging from 1 to 3 kg/100 m^2. At the center of the patch, the denser core spanned 1.8 km^2 and had a density of 2–3 kg/100 m^2. During this survey, images deletions led to areas without jellyfish estimation (Fig. 6). Two less dense patches were detected at the western and southern extremes of Bages-Sigean with areas of, respectively, 2.8 and 3.9 km^2 (7.4 and 10.3% of the lagoon) and smaller

Table 1
Characteristics of each flight analyzed images and biomass estimation. Images out of Bages-Sigean lagoon were not considered. The images used for the maps were filtered to have a frequency of waves inferior to the median of all flights.

Flight date	Altitude (m)	Area covered (Km^2) (% lagoon)	Number of pictures	Pictures with detected jellyfish (%total)	Pictures used for the analyses (%total)	Mean analyzed area/picture (km^2)	Mean medusae total length (cm)	Mean biomass per medusae (Kg)
12/07/22	612 ± 55	52.8 (100%)	3120	2635 (84%)	1918 (61%)	0.52 ± 0.01	30.5 ± 5.2	1.6 ± 0.6
31/08/22	260 ± 29	35.0 (92%)	2498	1805 (72%)	666 (26%)	0.03 ± 0.01	28.8 ± 5.7	1.4 ± 0.7
04/10/22	338 ± 40	42.2 (100%)	3663	3438 (93%)	1975 (54%)	0.03 ± 0.05	26.9 ± 6.1	1.2 ± 0.7

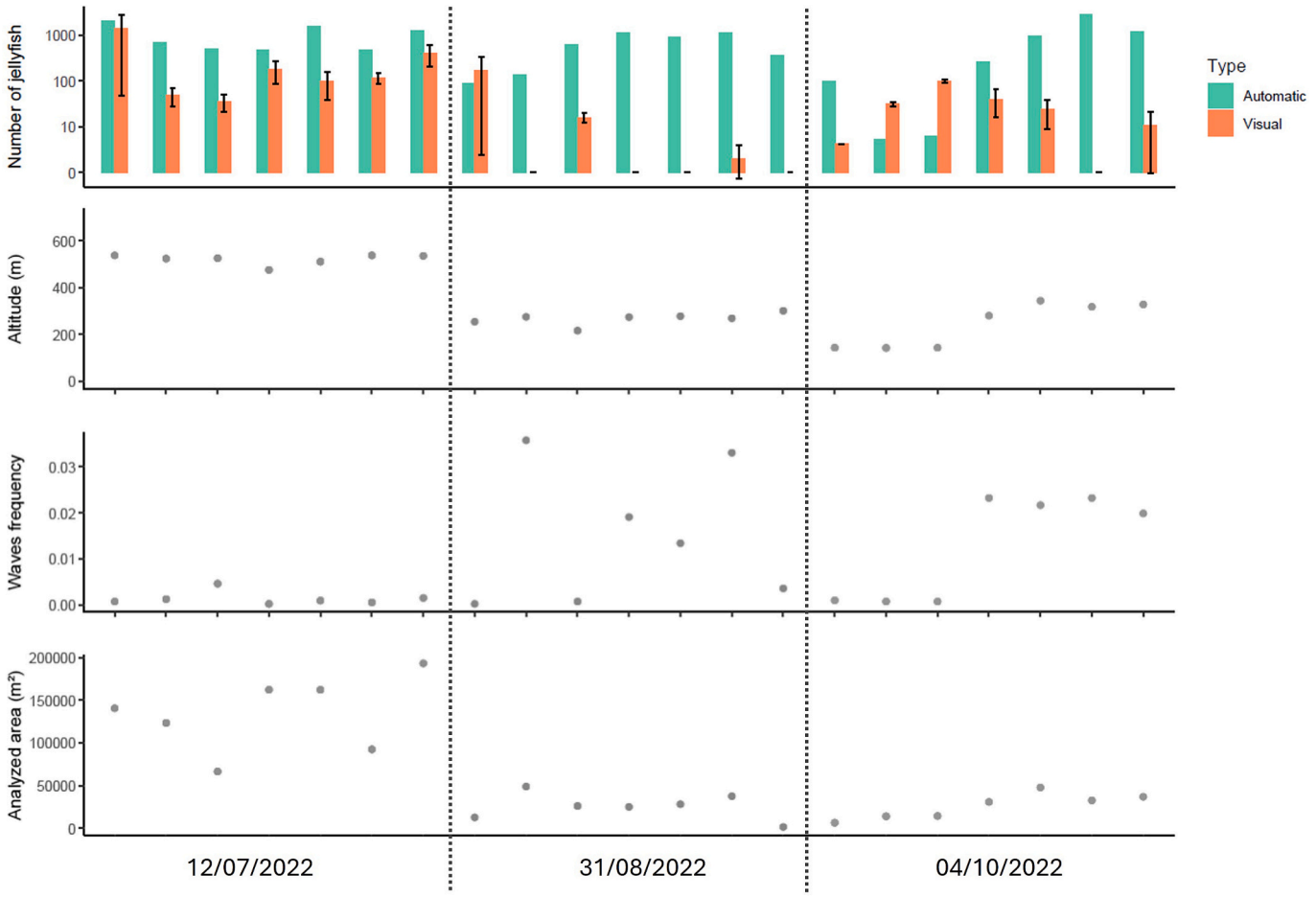

Fig. 5. Number of medusae visually counted in orange (mean ± sd between counters) vs. medusae automatically detected (in green) in images sampled from the three flights. Altitude (m), FFT peak value (cf. methods, section 2.3.4) and analyzed area (m^2) of each image are indicated. (For interpretation of the references to colour in this figure legend, the reader is referred to the web version of this article.)

densities below 1.8 kg/100 m^2.

By early October, jellyfish patches were more scattered than in previous surveys. The denser patch was in the eastern part of the lagoon, as in the first flight, covered an area of 1.5 km^2 with a density ranging from 1 to 3 kg/100 m^2. The density and area of the second main patch, in the western part, were reduced (1 to 2.5 kg/100 m^2, 0.7 km^2). Additionally, the six interconnected small patches (1 to 2 kg/100 m^2) covered a consequent area of about 10.2 km^2. In total, all the patches accounted for 32.6% of the lagoon (Fig. 6).

3.5. Cohorts

The multimodal analysis on the total length frequencies revealed two to three log normal distributions per flight (p-values <0.001), indicating the presence of four cohorts (Fig. 7). The first cohort was only detected in July, as individuals reached their maximum size of 30–40 cm by that time. The second cohort was the most abundant in July, spanning a wide size range from 20 to 40 cm. This cohort likely ended in late August, with individuals between 30 and 40 cm. The third cohort was present from July to October. Medusae under 20 cm of total length are detected in July, then mostly between 20 and 35 cm in August where they represent the main cohort. This cohort likely ended in October where most of the individuals exceed 30 cm of total length. The fourth and last cohort were only detected in October, with medusae ranging from under than 20 to 30 cm in total length (Fig. 7).

A VBGF was calculated for the third cohort as this is the only cohort whose individual's growth was observed across all three surveys. The growth coefficient was K = 5.18/year. The third cohort may have started

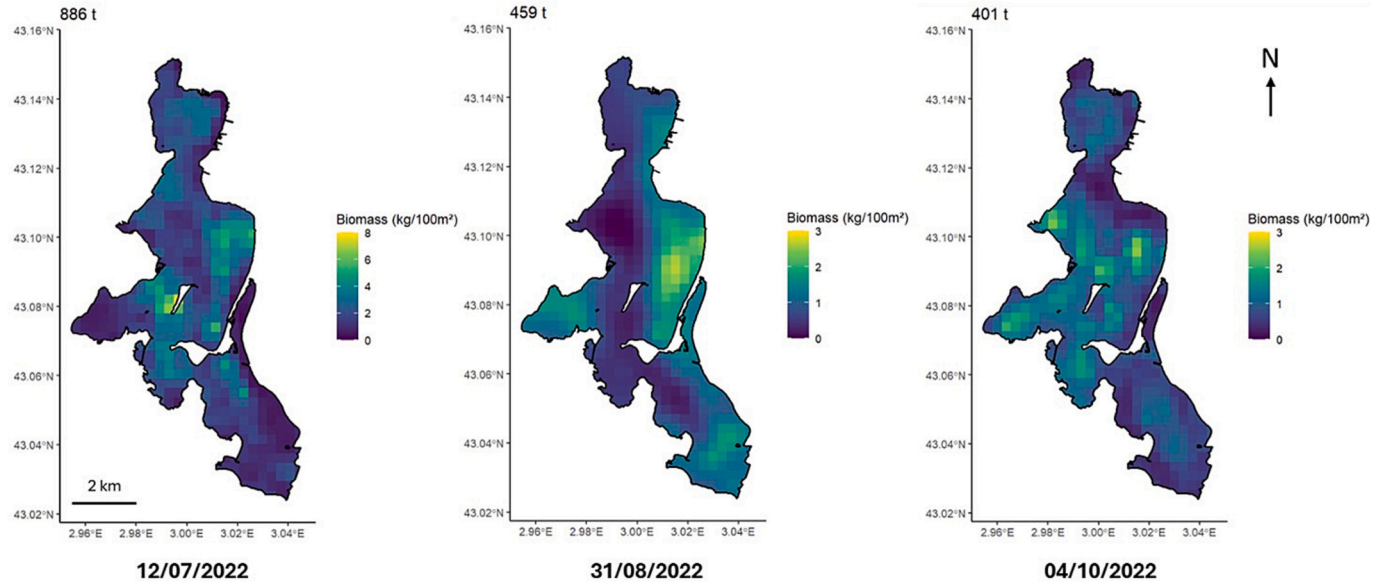

Fig. 6. Distribution of *R. pulmo* biomass (Kg/100m^2) and global biomass in Bages-Sigean lagoon through time. Grid of 300x300m.

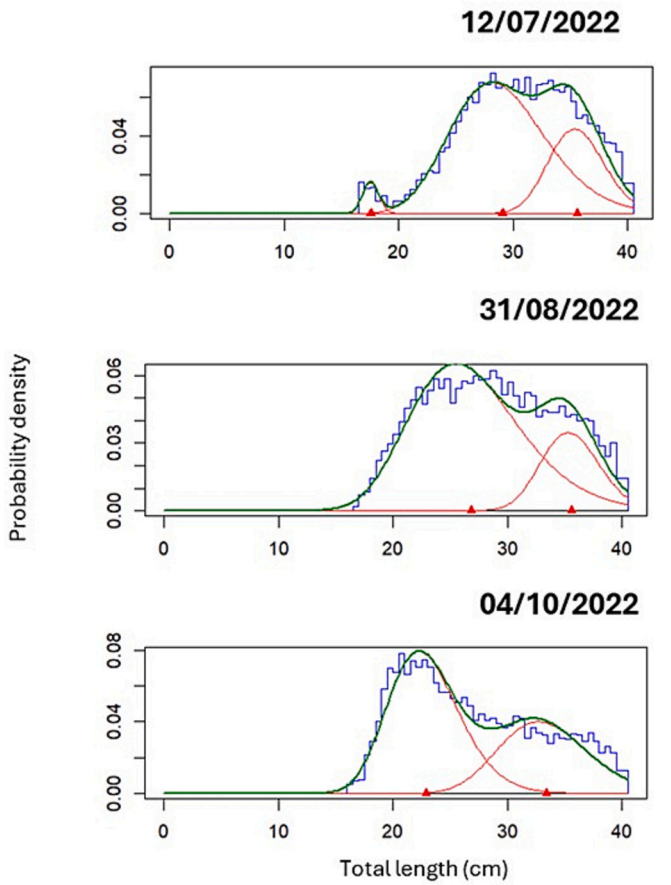

Fig. 7. Detection of cohorts through multimodal analysis on the distribution of total length (cm) across medusae population for each flight date: 12/07/2022, 31/08/2022 and 04/10/2022.

in May ($t_0 = 1.15$) and ended in October (Fig. 7).

4. Discussion

4.1. Methodological considerations: strengths and limitations of aerial surveys

The complete aerial coverage of the Bages-Sigean lagoon to monitor *Rhizostoma pulmo* blooms was achieved using a light plane, an approach that overcomes the spatial limitations of drones. The observed patches (1.5–6.1 km^2, or up to 32.6% of the lagoon surface) fall within the broad range reported for jellyfish aggregations worldwide but are relatively small compared with massive coastal blooms (Graham et al., 2003; Houghton et al., 2006). The aerial coverage of the whole lagoon in a single day represented a major logistical challenge, which justified the use of a plane instead of drones, whose limited autonomy restricts the area they can cover (Table 2; Schaub et al., 2018). Previous studies have similarly used small planes to survey jellyfish aggregations and have reported a spatial coverage spanning several km^2 (Graham et al., 2003; Houghton et al., 2006), whereas drones typically capture only relatively small patches (e.g. Schaub et al., 2018). Reported jellyfish patch sizes vary greatly across species and regions, for instance, *Aurelia* spp. patches have ranged from tens of m^2 in Alaska (Purcell et al., 2000) to several patches >314 m^2 (covering a total area of 2.35 km^2) in Japan (Uye et al., 2003), and Rhizostomeae aggregations have reached up to 150 km^2 for *P. punctata* in Lake Borgne (Graham et al., 2003) and 14–4600 km^2 for

Table 2
Review of the total area covered during jellyfish surveys using aerial imagery.

Total area covered	Aircraft	Altitude (m)	Species	Source
60 m transect	Drone	10	*Aurelia* sp.	Hamel et al., 2021
1750–2450 m^2	Drone	6–10	*Chironex fleckeri*	Rowley et al., 2020
75,000 m^2	Drone	70	*Catostylus mosaicus*	Raoult and Gaston, 2018
74,000–150,000 m^2 (22,459 ± 7541 m^2 × 5 sites)	Drone	6.7	*Cassiopea* sp.	Rowe et al., 2022
35,000,000–52,800,000 m^2	Plane	260–612	*Rhizostoma pulmo*	This study
> 150,000,000 m^2	Plane	100–325	*Phyllorhiza punctata*	Graham et al., 2003

R. octopus in the Irish Sea (Houghton et al., 2006). The relative smaller aggregations observed in this study ranging from 1.5 to 6.1 km^2 likely reflect the perennial, low-recruitment nature of the lagoon population, in contrast with the reported large coastal blooms in open ecosystems.

Aerial surveys are increasingly used to monitor jellyfish aggregations, often in combination with nets, boat transects, or acoustic methods to capture both horizontal and vertical distributions (Hamel et al., 2021; Purcell et al., 2000; Uye et al., 2003). Several non-invasive technologies such as acoustic and acoustic cameras have been demonstrated efficient to identify, detect and evaluate the density of jellyfish (Makabe et al., 2012; Wang et al., 2025). These approaches are particularly useful for determining the vertical distribution of jellyfish in the water column and for detecting small specimens, typically above 4 cm of diameter (Han and Uye, 2009; Makabe et al., 2012; Wang et al., 2025). However, applying such technologies at the scale of an entire lagoon would require the deployment of multiple sensors to ensure adequate spatial coverage. In the Bages–Sigean lagoon, this would have involved substantial logistical constraints and costs, especially given the presence of ongoing fishing and touristic activities. In contrast, the shallow depth of the lagoon (approximately 2 m) allows direct visualization of *Rhizostoma pulmo*, making high-altitude aerial surveys a practical and efficient approach for obtaining accurate abundance estimates over large spatial scales. Whole-lagoon coverage minimized the risk of over- or underestimation associated with discrete transects, which can inflate density estimates by several-fold due to patchiness (Rowe et al., 2022). Indeed, medusae patchy distribution creates strong density variations limiting the generalization of local measurements. Rowe et al. (2022) compared *Cassiopea* sp. medusae counts from boat visual transects, drone transects and drone covering entire sites. They concluded that the global density calculated from the transects was overinflated by more than 300% for drones transects and almost 200% for direct observations from boats transects, regarding the global density obtained by analyzing whole sites. In this study, the biomass determined from visual transects and estimated through image analysis were very different for the same area on 12/07/2022 (i.e. 0.11 and 0.02 kg/100 m^2 observed during transects 1 and 2 correspond to 3.2 and 1.8 kg/100 m^2 in the map). These discrepancies likely reflect the strong spatial heterogeneity of jellyfish distribution within the lagoon. Aerial survey grid cells represent areas of 300 × 300 m (0.09 km^2), whereas visual transects sample only narrow corridors (approximately 0.006 km^2). This interpretation is supported by hand-net sampling results, as no jellyfish were captured at the fixed station while aggregations were detected elsewhere in the lagoon. Therefore, covering the entire lagoon across multiple dates during the bloom provides a more reliable method than extrapolation from discrete local transects.

Automated image analysis further increased efficiency, processing >2000 images per flight. The choice of developing an AI-free code tailored to the images was driven by three key constraints: the quantity of pictures, the resolution due to high altitude, and the specificity of the masked area. Common methods for automatic detection and counts of medusae used in aerial surveys analysis include threshold-based image processing (Hamel et al., 2021) or image treatment software (Choi et al., 2021; Graham et al., 2003; Raoult and Gaston, 2018), as well as AI-based approaches (Mcilwaine and Casado, 2021). While image processing software allows for some threshold adjustments, it does not offer the level of specificity that a custom code based on the analyzed images can provide. Additionally, AI implementation would have required a high degree of certainty in manual jellyfish identification to train the model. Mcilwaine and Casado (2021) developed their convolutional neural network using images taken at relatively low altitude (100 m), where jellyfish identification certainty was high, which was not possible in our case given the substantially higher altitude of the flights over Bages-Sigean lagoon.

Evaluation of the algorithm performance, by comparison with manual counts, revealed the influence of surface ripples, altitude and sun glare, requiring careful filtering of images. Medusae abundance from aerial images yielded results comparable to those of nets or visual boats transects (Hamel et al., 2021; Rowe et al., 2022; Rowley et al., 2020), indicating that aerial monitoring is a valuable approach. In addition, automated detection and manual counts of the jellyfish were similar in Raoult and Gaston (2018) and Hamel et al. (2021), but these results derived from aerial images taken from drones at low altitude (Table 2). In this study, a significant difference between automatic and manual counts was detected from the analysis of images taken at high altitude (Fig. 5). Indeed, many environmental factors (e. g. waves, background heterogeneity, sun glare) can induce false positives. Accordingly, filters are applied to the images during the analysis (Choi et al., 2021; Hamel et al., 2021). Adapting flight schedules to favorable weather conditions, such as cloudy and windless days, may help mitigate these problems (Rowley et al., 2020; Schaub et al., 2018). Nevertheless, weather conditions in Bages-Sigean are, most of the time, windy and sunny. Technical solutions may be considered such as polarizing filters or adapting the camera angle (Schaub et al., 2018). High primary production might also reduce water clarity in lagoons, restraining consequently jellyfish detection. These results highlight both the potential and the limitations of aerial surveys: they provide robust large-scale coverage but remain sensitive to environmental conditions and require tailored analytical workflows.

4.2. Bloom biomass, seasonal dynamics and resource potential

Our results confirm a strong seasonal peak of *R. pulmo* biomass in July, with a marked decline in August and October. The sharp increase in temperature observed from April to June (exceeding 10 °C) may have triggered strobilation of *R. pulmo* polyps and the release of ephyrae. In addition, the first cohorts likely benefited from the chlorophyll-a peak observed in May–June, potentially enhancing zooplankton availability and thereby supporting jellyfish growth through bottom-up processes. The overall pattern of *R. pulmo* population dynamics broadly aligns with previous observations in the Bages–Sigean lagoon (Leoni et al., 2021), although the secondary autumn peak reported in 2019 was not observed in 2022. Such discrepancies reflect interannual variability in bloom dynamics underscoring the need for long-term monitoring.

Medusae biomass derived from aerial images are consistent with in situ observation, confirming that aerial surveys are a suitable method for estimating jellyfish biomass (Leoni et al., 2021). Raoult and Gaston (2018) considered the area of half of the ellipse of the spotted individuals as a proxy for the jellyfish diameter from which biomass was then estimated. In this study, a similar approach was applied, using the major axis of the detection ellipse to determine the total length of medusae for biomass calculations. Like *C. mosaicus* (Raoult and Gaston, 2018), *R. pulmo* mostly swims horizontally, parallel to the surface. Given that the lagoon is shallow and the visibility high, the entire bloom's biomass could be estimated from a single flight, overcoming the challenges posed by the high spatial and temporal variability of jellyfish.

Estimated total biomass ranged from 401 to 886 t, with values halving within three months. This decline likely reflects both natural mortality and a progressive reduction in medusae size, consequences of their sexual reproduction (Leoni et al., 2021). Individuals under 10 cm were not considered in the analysis and therefore the biomass is underestimated. During the field sampling, individuals under 10 cm were observed only in transects on the 12/07/2022. They represented 2% of the total biomass, accounting for 18 t of the total biomass estimate in the lagoon through imagery on the same date. Compared with other regions, biomass levels in Bages-Sigean were higher than those reported for *R. octopus* in Carmarthen Bay (40–594 t; Elliott et al., 2017), and the 347 t of *Catostylus mosaicus* in Smiths Lake (Australia, Raoult and Gaston, 2018). However, they represent only 5% of the massive *P. punctata* aggregations in the Gulf of Mexico (~19,300 t; Graham et al., 2003). Thus, *R. pulmo* blooms in the lagoon fall within the global range of Rhizostomeae biomass values, while reflecting the unique dynamics of a perennial, lagoon-based population.

Rhizostomeae jellyfish are commercialized for applications in pharmaceuticals and biomedicals fields or for food (Leone et al., 2015; Brotz et al., 2024). *R. pulmo* contains many compounds of interest to these industries, especially collagen, but also antioxidant peptides and other bioactive molecules, as the market for jellyfish as a food item is not developed in Europe (Leone et al. 2015; Brotz et al., 2024). Artisanal fisheries are already present in Bages-Sigean thus harvesting jellyfish when they are massively present in summer could represent an interesting complementary activity for fishermen. As medusae are produced by polyps which will not be harvested, *R. pulmo* stock management could, at first sight, be considered as simple considering that fishing all the pelagic population will not impact the production of the year after. However, estimating sustainable catch volumes is not yet possible since perspective on jellyfish long-term dynamics is lacking; for example, while many scyphozoan species present asexual reproduction strategies with budding and high substrate colonization rate, *R. pulmo* polyps tend not to expand in large colonies and, in contrary, are embedded. The fragility of those benthic populations is still to be studied and therefore no prediction can yet be made on stock sustainability. This evaluation of their biomass in the lagoon at large scale was never done before and could represent a first step to assessing their rentability. The amount of *R. pulmo* present in the lagoon might be of interest for fisheries, however, extreme interannual variations may occur in jellyfish populations (Brotz, 2016; Thibault et al., 2024). This underscores the need for long-term monitoring and a better understanding of the species life cycle before considering any fishery activity (Brotz, 2016). For instance, while *R. pulmo* have been harvested in Turkey for 22 years, the fishery faced collapse due to the strong variation in landings (0–4000 t/year) and the inability to predict jellyfish blooms (Brotz, 2016).

4.3. Cohort structure and population growth

Aerial monitoring revealed the presence of four *R. pulmo* cohorts in 2022, while the presence of a fourth cohort was only suggested in 2019 (Leoni et al., 2021); this dynamic is consistent with observations from the Mar Menor (Fernández-Alías et al., 2020). Cohort timing corresponded closely between 2019 and 2022, likely reflecting comparable environmental conditions, with temperatures, salinity and Chlorophyll within similar ranges for both years (Fig. 4; Leoni et al., 2021). The first cohort started before July, as adult individuals (total length > 15 cm) were detected during the first flight, consistent with Leoni et al. (2021), who identified the first juveniles (< 15 cm) in April. The similar phenology of *R. pulmo* 2019 and 2022 cohorts suggests similar VBGF values. Growth analysis revealed an asymptotic size of 40 cm and a growth coefficient of 5.18 per year, comparable to values reported for the first cohort of *R. pulmo* in 2019 ($K = 4.47$ per year, $L_{inf} = 40.95$ cm; Leoni et al., 2021) and other Rhizostomeae such as *P. punctata* ($K = 4.69$ per year; Garcia and Durbin, 1993 in Palomares and Pauly, 2008). These consistencies support the reliability of cohort detection from aerial imagery. In addition to the VBGF, the growth rate calculated for the third *R. pulmo* cohort of 2022 (1.86 mm/day) falls within the growth rates observed for the 2019 cohorts: 1.5–2.3 mm/day (Leoni et al., 2021), confirming the reliability of the aerial survey for growth rate assessment. However, some limitations remain: only three sampling dates were available in our study and individuals under 10 cm were undetectable. Adjustment to the protocol such as flying at lower altitudes, using a camera objective with a higher resolution (e.g. 80 or 110 mm instead of 55), and increasing the frequency of flights, could improve the detection of smaller individuals and enhance cohort monitoring accuracy. Furthermore, estimated biomass density could not have been calibrated with field sampling and must therefore be approached with caution. In addition, the bloom onset still requires in situ monitoring either through polyps' strobilation (which has not yet been observed in the field for *R. pulmo*) or the first pelagic stages (e.g. ephyrae), which cannot be detected via aerial imagery due to their size (< 1 cm). Consequently, integrating in situ sampling with aerial monitoring remains essential for linking strobilation events to cohort formation, as well as evaluating biomass estimation accuracy.

5. Conclusion and perspectives

The aerial survey of *R. pulmo* in Bages-Sigean lagoon has proven to be an efficient and robust method for monitoring jellyfish biomass and cohorts' dynamics throughout the blooming season. By providing rapid, non-invasive and detailed data on medusae size and distribution, aerial survey complements traditional methods such as nets and boats surveys. These advantages highlight the potential of the aerial approach for stock assessment of medusae, both for exploitation and ecological purposes. The method is particularly powerful in shallow systems, where direct visualization is possible, and where whole-site coverage can minimize the biases of traditional local transects. However, this approach is constrained by environmental conditions, flight altitude, limited ability to detect early life stages, and high operational costs.

Future directions should include integrating aerial surveys with complementary tools, such as simultaneous net monitoring, acoustic methods, and AI-based image recognition, while building long-term time series. Applying Deep Learning approaches to aerial image analysis could improve jellyfish detection accuracy and potentially allow faster processing of new images once the model is trained. Although this was beyond the scope of the present study, comparing AI-based results with traditional methods could provide valuable insights into optimal approaches for analyzing aerial images of jellyfish blooms, particularly under varying environmental conditions and depending on the study objectives. Such efforts are critical not only for advancing ecological understanding of jellyfish bloom dynamics and evaluating their potential as a sustainable bioresource.

CRediT authorship contribution statement

Marie Meffre: Writing – review & editing, Writing – original draft, Visualization, Validation, Software, Methodology, Investigation, Formal analysis, Data curation, Conceptualization. **Yann Tremblay:** Writing – review & editing, Visualization, Software, Methodology, Investigation, Data curation. **Anaïs Courtet:** Writing – review & editing, Investigation. **Etienne Bourgouin:** Writing – review & editing, Investigation. **Juan-Carlos Molinero:** Writing – review & editing, Supervision, Formal analysis. **Delphine Bonnet:** Writing – review & editing, Visualization, Validation, Supervision, Resources, Project administration, Methodology, Investigation, Funding acquisition, Data curation, Conceptualization.

Declaration of competing interest

The authors declare that the research was conducted in the absence of any commercial or financial relationships that could be construed as a potential conflict of interest.

Acknowledgements

MM was funded by the Aquarium de Paris. The research was carried out within the framework of the RITHM project (PI: DB- Aerial surveys) from the Key initiative Sea and Coast of Montpellier University of Excellence and the LabCom Jellyfih and Polyps Academy ANR-23-LCV2-0013-01. We are grateful to the Sub-C Marine society for the aerial surveys and the images acquisition.

Data availability

A subset of the data analyzed in the study and the codes used to process them can be found online at https://zenodo.org/records/19089350. All the aerial images could not be deposited in the repository due to the size of the files; however, these data will be

made available on request.

References

Brotz, L., 2016. Jellyfish Fisheries of the World (Doctoral dissertation, University of British Columbia). 180p.

Brotz, L., Angel, D.L., D'Ambra, I., Enrique-Navarro, A., Lauritano, C., Thibault, D., Prieto, L., 2024. Rhizostomes as a resource: the expanding exploitation of jellyfish by humans. Adv. Mar. Biol. 98, 511–547. https://doi.org/10.1016/bs.amb.2024.08.001.

Chen, Y., Zhang, R., Ge, Y., Jin, Y., Xia, Z., 2019. Downscaling census data for gridded population mapping with geographically weighted area-to-point regression kriging. Ieee Access 7, 149132–149141. https://doi.org/10.1109/ACCESS.2019.2945000.

Choi, S.Y., Kim, H.J., Seo, M.H., Soh, H.Y., 2021. Density estimation of *Nemopilema nomurai* (Scyphozoa, Rhizostomeae) using a drone. J. Indian Soc. Remote Sens. 49, 1727–1732. https://doi.org/10.1007/s12524-021-01347-0.

Churnside, J.H., Marchbanks, R.D., Donaghay, P.L., Sullivan, J.M., Graham, W.M., Wells, R.D., 2016. Hollow aggregations of moon jellyfish (*Aurelia* spp.). J. Plankton Res. 38 (1), 122–130. https://doi.org/10.1093/plankt/fbv092.

Correia, C.A., Andrade, F.A., Sivertsen, A., Guedes, I.P., Pinto, M.F., Manhães, A.G., Haddad, D.B., 2022. Comprehensive direct georeferencing of aerial images for unmanned aerial systems applications. Sensors 22 (2), 604. https://doi.org/10.3390/s22020604.

D'Ambra, I., Merquiol, L., 2022. Jellyfish from fisheries by-catches as a sustainable source of high-value compounds with biotechnological applications. Mar. Drugs 20 (4), 266. https://doi.org/10.3390/md20040266.

de Lamarck, J.-B.M., 1816. Histoire naturelle des animaux sans vertèbres. Tome second, 566 pp. Verdière, Paris.

Duarte, I.M., Marques, S.C., Leandro, S.M., Calado, R., 2022. An overview of jellyfish aquaculture: for food, feed, pharma and fun. Rev. Aquac. 14, 265–287. https://doi.org/10.1111/raq.12597.

Elliott, A., Hobson, V., Tang, K.W., 2017. Balancing fishery and conservation: a case study of the barrel jellyfish *Rhizostoma octopus* in South Wales. ICES J. Mar. Sci. 74 (1), 234–241. https://doi.org/10.1093/icesjms/fsw157.

Fernández-Alías, A., Marcos, C., Pérez-Ruzafa, A., 2024. The unpredictability of scyphozoan jellyfish blooms. Front. Marine Sci. 11, 1349956. https://doi.org/10.3389/fmars.2024.1349956.

Fernández-Alías, A., Marcos, C., Quispe, J.I., Sabah, S., Pérez-Ruzafa, A., 2020. Population dynamics and growth in three scyphozoan jellyfishes, and their relationship with environmental conditions in a coastal lagoon. Estuar. Coast. Shelf Sci. 243, 106901. https://doi.org/10.1016/j.ecss.2020.106901.

Fleming, N.E., Harrod, C., Houghton, J.D., 2013. Identifying potentially harmful jellyfish blooms using shoreline surveys. Aquac. Environ. Interact. 4 (3), 263–272. https://doi.org/10.3354/aei00086.

Gao, M., Bai, Y., Li, Z., Li, S., Zhang, B., Chang, Q., 2021. Real-time jellyfish classification and detection based on improved YOLOV3 algorithm. Sensors 21 (23), 8160. https://doi.org/10.3390/s21238160.

Gmelin, J.F., 1791. Vermes. In: Gmelin, J.F. (Ed.), Caroli a Linnaei Systema Naturae per regna Tria Naturae, Ed. 13. Tome 1(6). G.E. Beer, Lipsiae, Leipzig. Systema Naturae, pp. 3021–3910. Linneaeus (ed.). Ed. 13. 1: pars. 6.

Graham, W.M., Martin, D.L., Felder, D.L., Asper, V.L., Perry, H.M., 2003. Ecological and economic implications of a tropical jellyfish invader in the Gulf of Mexico. Biol. Invasions 5, 53–69. https://doi.org/10.1023/A:1024046707234.

Graham, W.M., Gelcich, S., Robinson, K.L., Duarte, C.M., Brotz, L., Purcell, J.E., Madin, L.P., Mianzan, H., Sutherland, K.R., Uye, S., Pitt, K.A., Lucas, C.H., Bøgeberg, M., Brodeur, R.D., Condon, R.H., 2014. Linking human well-being and jellyfish: ecosystem services, impacts, and societal responses. Front. Ecol. Environ. 12 (9), 515–523. https://doi.org/10.1890/130298.

Gray, P.C., Bierlich, K.C., Mantell, S.A., Friedlaender, A.S., Goldbogen, J.A., Johnston, D. W., 2019. Drones and convolutional neural networks facilitate automated and accurate cetacean species identification and photogrammetry. Methods Ecol. Evol. 10, 1490–1500. https://doi.org/10.1111/2041-210X.13246.

Hamel, H., Lhoumeau, S., Wahlberg, M., Javidpour, J., 2021. Using drones to measure jellyfish density in shallow estuaries. J. Mar. Sci. 9 (6), 659. https://doi.org/10.3390/jmse9060659.

Han, C.H., Uye, S.I., 2009. Quantification of the abundance and distribution of the common jellyfish *Aurelia aurita s.l.* with a dual-frequency IDentification SONar (DIDSON). J. Plankton Res. 31 (8), 805–814. https://doi.org/10.1093/plankt/fbp029.

Hamner, W.M., Dawson, M.N., 2009. A review and synthesis on the systematics and evolution of jellyfish blooms: advantageous aggregations and adaptive assemblages. Hydrobiologia 616 (1), 161–191. https://doi.org/10.1007/s10750-008-9620-9.

Han, Y., Chang, Q., Ding, S., Gao, M., Zhang, B., Li, S., 2022. Research on multiple jellyfish classification and detection based on deep learning. Multimed. Tools Appl. 1–16. https://doi.org/10.1007/s11042-021-11307-y.

Houghton, J.D., Doyle, T.K., Davenport, J., Hays, G.C., 2006. Developing a simple, rapid method for identifying and monitoring jellyfish aggregations from the air. Mar. Ecol. Prog. Ser. 314, 159–170. https://doi.org/10.3354/meps314159.

Kim, H., Koo, J., Kim, D., Jung, S., Shin, J.U., Lee, S., Myung, H., 2016. Image-based monitoring of jellyfish using deep learning architecture. IEEE Sensors J. 16 (8), 2215–2216. https://doi.org/10.1109/JSEN.2016.2517823.

Kishinouye, K., 1922. Echizen kurage. Zool. Mag. 34, 343–346.

Lee, S.H., Tseng, L.C., Yoon, Y.H., Ramirez-Romero, E., Hwang, J.S., Molinero, J.C., 2023. The global spread of jellyfish hazards mirrors the pace of human imprint in the marine environment. Environ. Int. 171, 107699. https://doi.org/10.1016/j.envint.2022.107699.

Leone, A., Lecci, R.M., Durante, M., Meli, F., Piraino, S., 2015. The bright side of gelatinous blooms: Nutraceutical value and antioxidant properties of three Mediterranean jellyfish (Scyphozoa). Mar. Drugs 13 (8), 4654–4681. https://doi.org/10.3390/md13084654.

Leoni, V., Molinero, J.C., Meffre, M., Bonnet, D., 2021. Variability of growth rates and thermohaline niches of *Rhizostoma pulmo's* pelagic stages (Cnidaria: Scyphozoa). Mar. Biol. 168 (7), 107. https://doi.org/10.1007/s00227-021-03914-y.

Linnaeus, C., 1758. Systema Naturae per regna tria naturae, secundum classes, ordines, genera, species, cum characteribus, differentiis, synonymis, locis. In: The System of Nature Through the Three Kingdoms of Nature, According to Classes, Orders, Genera, Species, With Characters, Differences, Synonyms, Places. Impensis Direct. Laurentii Salvii, Holmiae, Stockholm, 824 p.

Macri, S., 1778. Nuove Osservazioni intorno la storia naturale del Polmone Marino degli Antichi, 36pp.

Makabe, R., Kurihara, T., Uye, S.I., 2012. Spatio-temporal distribution and seasonal population dynamics of the jellyfish *Aurelia aurita* sl studied with dual-frequency IDentification SONar (DIDSON). J. Plankton Res. 34 (11), 936–950. https://doi.org/10.1093/plankt/fbs057.

Mariani, P., 2018. Jellyfish identification software for underwater laser cameras (JTRACK). Res. Ideas Outcomes 4, e24716. https://doi.org/10.3897/rio.4.e24716.

McGeady, R., Runya, R.M., Dooley, J.S., Howe, J.A., Fox, C.J., Wheeler, A.J., Summers, G., Callaway, A., Beck, S., Brown, S.L., Dooly, G., McGonigle, C., 2023. A review of new and existing non-extractive techniques for monitoring marine protected areas. Front. Mar. Sci. 10, 1126301. https://doi.org/10.3389/fmars.2023.1126301.

Mcilwaine, B., Casado, M.R., 2021. JellyNet: the convolutional neural network jellyfish bloom detector. Int. J. Appl. Earth Obs. Geoinf. 97, 102279. https://doi.org/10.1016/j.jag.2020.102279.

Nagata, R.M., D'Ambra, I., Lauritano, C., von Montfort, G.M., Djeghri, N., Jordano, M.A., Colin, P.S., Costello, H.J., Leoni, V., 2024. Physiology and functional biology of Rhizostomeae jellyfish. Adv. Mar. Biol. 98, 255–360. https://doi.org/10.1016/bs.amb.2024.07.007.

Oliver, M.A., Webster, R., 1990. Kriging: a method of interpolation for geographical information systems'. Int. J. Geogr. Inf. Syst. 4 (3), 313–332. https://doi.org/10.1080/02693799008941549.

Palomares, M.L.D., Pauly, D., 2008. The growth of jellyfishes. In: Jellyfish Blooms: Causes, Consequences, and Recent Advances: Proceedings of the Second International Jellyfish Blooms Symposium, Held at the Gold Coast, Queensland, Australia, 24–27 June, 2007. Springer Netherlands, Dordrecht, pp. 11–21. https://doi.org/10.1007/978-1-4020-9749-2_2.

Purcell, J.E., 2009. Extension of methods for jellyfish and ctenophore trophic ecology to large-scale research. Hydrobiologia 616, 23–50. https://doi.org/10.1007/s10750-008-9585-8.

Purcell, J.E., Brown, E.D., Stokesbury, K.D., Haldorson, L.H., Shirley, T.C., 2000. Aggregations of the jellyfish *Aurelia labiata*: abundance, distribution, association with age-0 walleye Pollock, and behaviors promoting aggregation in Prince William sound, Alaska, USA. Mar. Ecol. Prog. Ser. 195, 145–158. https://doi.org/10.3354/meps195145.

Quoy, J.R.C., Gaimard, J.P., 1824-1826. Zoologie. In: de Freycinet, L. (Ed.), Voyage au tour du monde fait par ordre du roi, sur les corvettes de S. M: l'Uranie et la Physicienne pendant les années 1817 à 1820 iv + 712 pp.

Raoult, V., Gaston, T.F., 2018. Rapid biomass and size-frequency estimates of edible jellyfish populations using drones. Fish. Res. 207, 160–164. https://doi.org/10.1016/j.fishres.2018.06.010.

Richardson, A.J., Bakun, A., Hays, G.C., Gibbons, M.J., 2009. The jellyfish joyride: causes, consequences and management responses to a more gelatinous future. Trends Ecol. Evol. 24 (6), 312–322. https://doi.org/10.1016/j.tree.2009.01.010.

Rowe, C.E., Figueira, W.F., Kelaher, B.P., Giles, A., Mamo, L.T., Ahyong, S.T., Keable, S. J., 2022. Evaluating the effectiveness of drones for quantifying invasive upside-down jellyfish (*Cassiopea* sp.) in Lake Macquarie, Australia. PLoS One 17 (1), e0262721. https://doi.org/10.1371/journal.pone.0262721.

Rowley, O.C., Courtney, R.L., Browning, S.A., Seymour, J.E., 2020. Bay watch: using unmanned aerial vehicles (UAV'S) to survey the box jellyfish *Chironex fleckeri*. PLoS One 15 (10), e0241410. https://doi.org/10.1371/journal.pone.0241410.

Ruiz-Frau, A., Martin-Abadal, M., Jennings, C.L., Gonzalez-Cid, Y., Hinz, H., 2022. The potential of Jellytoring 2.0 smart tool as a global jellyfish monitoring platform. Ecol. Evol. 12 (11), e9472. https://doi.org/10.1002/ece3.9472.

Schaub, J., Hunt, B.P., Pakhomov, E.A., Holmes, K., Lu, Y., Quayle, L., 2018. Using unmanned aerial vehicles (UAVs) to measure jellyfish aggregations. Mar. Ecol. Prog. Ser. 591, 29–36. https://doi.org/10.3354/meps12414.

Southcott, R.V., 1956. Studies on Australian Cubomedusae, including a new genus and species apparently harmful to man. Mar. Freshw. Res. 7 (2), 254–280. https://doi.org/10.1071/MF9560254.

Thibault, D., Kuplik, Z., Prieto, L., Enrique-Navarro, A., Brown, M., Uye, S., Doyle, T., Pitt, K., Fitt, W., Gibbons, M., 2024. Ecology of Rhizostomeae. Adv. Mar. Biol. 98, 397–509. https://doi.org/10.1016/bs.amb.2024.07.008.

Uye, S.I., 2011. Human forcing of the copepod–fish–jellyfish triangular trophic relationship. Hydrobiologia 666, 71–83. https://doi.org/10.1007/s10750-010-0208-9.

Uye, S.I., Fujii, N., Takeoka, H., 2003. Unusual aggregations of the scyphomedusa *Aurelia aurita* in coastal waters along western Shikoku, Japan. Plankton Biol. Ecol. 50 (1), 17–21.

von Lendenfeld, R., 1884. The scyphomedusae of the southern hemisphere. Part III. Proc. Linnean Soc. NSW 9, 259–306.

Wang, B., Liu, X., Dong, J., Wang, A., Feng, C., Xu, Y., Zhang, D., Zhao, Z., 2025. Evaluating the effectiveness of an acoustic camera for monitoring three large jellyfish species in the coastal waters of Liaodong Bay, China. Fishes 10 (3), 105. https://doi.org/10.3390/fishes10030105.

Webster, R., Oliver, M.A., 2007. Geostatistics for Environmental Scientists. John Wiley and Sons, 309p.

Xiaobin, W., Hongkai, Z., Yudi, Z., Fang, Z., Peituo, X., Qun, L., Chong, L., Dong, L., 2021. Characteristics of jellyfish in the Yellow Sea detected by polarized oceanic lidar. Infrared Laser Eng. 50 (6). https://doi.org/10.3788/IRLA20211038, 20211038–1.